Available online at www.sciencedirect.com
SCIENCE DIRECT®
ELSEVIER
European Journal of Mechanics B/Fluids 22 (2003) 279–290
EUROPEAN JOURNAL OF MECHANICS B/FLUIDS

Experiments on control of streamwise streaks

Fredrik Lundell, P. Henrik Alfredsson *

KTH Mechanics, 100 44 Stockholm, Sweden

Received 9 September 2002; accepted 10 March 2003

Abstract

Control of streamwise velocity streaks are studied experimentally in a plane channel flow. High and low-velocity streaks are created by suction through streamwise slots and, further downstream, the secondary instability of the streaks is forced by speakers. The streaks are controlled by localized suction downstream of the disturbance generation. In a modified setup, reactive control is used in order to delay transition of low-velocity regions appearing at known spanwise positions randomly in time. As expected, the growth rate of the secondary instability decreases when localized suction is applied below a low-velocity streak. With control applied, transition is substantially delayed. The suction position and, in the case of reactive control of randomly appearing disturbances, the time instants at which control suction was turned on/off, were varied. The parameter study shows that the control suction has to be applied within a narrow region (10% of a streak width) around the centre of a low-velocity streak. The timing of the control suction is seen to be less critical.
© 2003 Éditions scientifiques et médicales Elsevier SAS. All rights reserved.

1. Introduction

For wall bounded flows, as, e.g., flow along vehicles (ships, airplanes) or in piping systems, skin friction drag can be the major source for the resistance to be overcome by the propulsion system. This has led to various proposals on how to decrease the drag. Examples in the past are for liquid flows polymer additives and microbubbles, whereas boundary-layer suction, cooling (or heating) the surface, Large Eddy Break Up-devices (LEBU:s) or grooved surfaces have been proposed for flows independent of the fluid. These methods are all distributed, in the sense that the full flow is affected. This is in contrast to selective methods which aim at control of specific and thereby localized (in time and space) events or structures. During the last ten years ideas have been presented based on local reactive control, where the idea is to detect and then selectively use control on flow structures which are identified to be responsible for transition to turbulence or turbulence production.

Several reviews [1–3] have been published recently describing the developments within the area of control. The development of refined control methods have mainly been done from a theoretical/numerical viewpoint and much less from a viewpoint of physical implementation. Most studies aim at controlling T-S waves or turbulent boundary layers. T-S waves may be controlled by periodic suction/blowing through a spanwise slot or heating a strip out-of-phase with the wave. When trying to control turbulent boundary-layer flows one focuses on the streamwise-oriented structures of high and low-velocity streaks in the near-wall region which are assumed to be the starting point for the bursting sequence. Usually the idea is to decrease the spanwise variation of streamwise velocity and thereby decrease the number or strength of the bursting sequences. This can be achieved by lozalized suction below low-velocity streaks and blowing below high-velocity streak.

In this context it is interesting to note that laminar-turbulent transition of boundary layers influenced by free-stream turbulence (FST) is preceded by the growth of streaky structures in the boundary layer (e.g., [4–6]). These streaks are the result of three-dimensional disturbances growing transiently in the boundary layer. The transient disturbance growth is due to non-orthogonality of the eigenmodes, which may give rise to large disturbance growth even at subcritical Reynolds numbers

* Corresponding author.
E-mail address: hal@mech.kth.se (P.H. Alfredsson).

0997-7546/03/$ – see front matter © 2003 Éditions scientifiques et médicales Elsevier SAS. All rights reserved.
doi:10.1016/S0997-7546(03)00032-3

[7–9]. It has been proposed that the growth mechanism behind the streaks in FST-induced transition is similar to the mechanism giving rise to streaks close to the wall in turbulent flows [10], and therefore plays a key role also in self-sustained turbulence [11].

An investigation of streamwise streaks was made by Elofsson, Kawakami and Alfredsson [12] in a model experiment in which streaks were created in a laminar Poiseuille channel flow. They concentrated on the secondary instability which develops on the streaks and found that the most unstable mode of the secondary wave instability was anti-symmetric with a wavenumber slightly smaller than the spanwise wavenumber of the streak. This is consistent with the analysis for streaks in a boundary layer performed by Andersson, Brandt and Henningson [13]. The theoretical results show that the secondary instability originates from the inflectional spanwise velocity profile developing as the streaks grow. The experimental findings of Elofsson, Kawakami and Alfredsson [12] support this conclusion for the streaks in the channel. After the growth of the secondary instability waves, incipient spots are seen to appear and further downstream, the flow becomes fully turbulent.

1.1. Experimental and numerical flow control

The results discussed above show that a control strategy which could be successful for boundary-layer control is one where the streaky structures are affected by the control. Localized suction has been used in order to decrease the growth of streamwise vortices or to control bursting events by, e.g., Myose and Blackwelder [14] (controlling streamwise Görtler vortices) and Gad-el-Hak and Blackwelder [15] (controlling artificially generated bursts). Bakchinov et al. [16] controlled transiently growing disturbances in a boundary layer by localized suction and blowing. A demonstration of a different control concept is Breuer, Haritonidis and Landahl [17], who used an array of moving wall elements to cancel a disturbance introduced by an initial wall movement (in the opposite direction from the one used for cancellation). All these studies aimed at, and suceeded in, delaying transition by acting locally on artificially generated structures in the flow.

For reactive control, localized sensing of the status of the flow is also necessary. For practical reasons wall information is usually the only possible alternative, either in form of the wall pressure or the shear stress. An example is the study by Fan, Herbert and Haritonidis [18], where a neural network was trained to give a phaseshift of the signal from a sensing microphone to the actuating speaker, minimizing pressure fluctuations at the wall downstream of the actuator.

Rathnasingham and Breuer [19] used pulsating jets driven by a resonance cavity in order to generate vortices inhibiting the bursting in a turbulent boundary layer. In the experiments, a linear system identification scheme was used in order to determine when and with what amplitude to turn on the actuators utilizing the information from upstream wall-wire sensors. Pressure sensors at the wall downstream of the actuating jets were used to tune the system. In the turbulent boundary layer under study, estimations from the mean-velocity profile show a shear-stress reduction of up to 7%. A blowing jet created by a piston-type actuator was used by Rebeck and Choi [20] and reduced the strength of the sweep motion towards the wall during bursts. An actuator, consisting of a moving beam above a cavity in the wall, can generate streamwise vortex structures. Such an actuator was constructed by Jacobsson and Reynolds [21]. Properly applied the actuator was shown to decrease the strength of streamwise structures in a boundary layer. They used wall-mounted hot films as sensors and showed successful control of streamwise vortices and streaks.

Choi, Moin and Kim [22] performed numerical simulations in which a proportional control scheme was used in order to decrease the strength of streaks in turbulent channel flows. In a numerical simulation the limitations of physical sensors and actuators are not present and in this case the control algorithm used the normal velocity at a certain height over the wall, prescribing the opposite of this velocity at the wall. Later simulations by Lee et al. [23] show that a neural network trained on the same problem adopted the same kind of control. Reductions in shear stress of up to 25% were obtained. By coupling the velocity at a specific height over the wall to the pressure variations at the wall, it will be possible to use wall-mounted pressure sensors in a physical implementation.

A general result from the studies above is that a complicated control algorithm based on system identification (using neural networks or linear system identification) does not show better results than the ones obtained with simple proportional controllers. It is also obvious that the typical physical implementation and the cases studied numerically differ in the sense that the physical implementation utilizes a limited number of sensors and actuators, whereas numerical studies may use information from all over the wall (or in the whole flow field) together with proper actuator output over the whole wall area (or in the whole flow field). In order for the knowledge from numerical/theoretical studies to be useful for physical implementation of reactive control, the theoretical/numerical knowledge needs to be complemented with physical or numerical experiments exploring the limitations of physically realizable actuators. On the other hand progress in sensor and actuator manufacturing has given a hope to produce a large number of sensors and actuators allowing individual structures in the flow to be controlled [24,25].

1.2. Present work

In this paper we attempt to describe how breakdown to turbulence in a model flow with streaky structures resembling that of a boundary layer subjected to free-stream turbulence or the near-wall region of a turbulent boundary layer, i.e., flow with

streamwise orientated regions of high and low velocity, can be delayed in a physical experiment. The experimental situation is similar to the one of Elofsson et al. [12]. In this setup, the effects of the control could be measured in a detailed manner. Also, the parameter space in which the control is effective was studied. Together with the knowledge of the disturbance structure in the boundary layer, the experiences from the model experiment will be used in order to design a control system for boundary layers subjected to FST, similar to the systems described above but comprising a larger number of sensors and actuators.

In Section 2, the experimental apparatus and in Section 3, experiments on the control of velocity streaks by localized suction are described. First, fundamental studies of the control are reported and after that, reactive control of randomly generated disturbances is presented. Finally, the results are summarized in Section 4.

2. Experimental setup

2.1. Flow apparatus

An open Poiseuille air-flow channel, consisting of two glass plates separated 8.2 mm by aluminum bars was used for the experiments. The flow was driven by a centrifugal fan, feeding the air through the channel via a muffler and a stagnation chamber and finally discharging out into the laboratory. Before entering the channel, the flow passed two turbulence damping-screens and a contraction. In Fig. 1 two setups are shown: (a) shows the setup used for fundamental studies of streak control and (b) the setup used for reactive control. Fig. 2 shows the block diagram of the reactive control experiment.

The coordinates are x (streamwise), y (vertical) and z (spanwise). All lengths are normalized with the half channel-height h (4.1 mm) and the velocity is scaled by the centreline velocity, U_{CL}. The channel walls are at $y = \pm 1$. The Reynolds number is defined as $\mathrm{Re} = U_{CL}h/\nu$ where ν is the kinematical viscosity of the air.

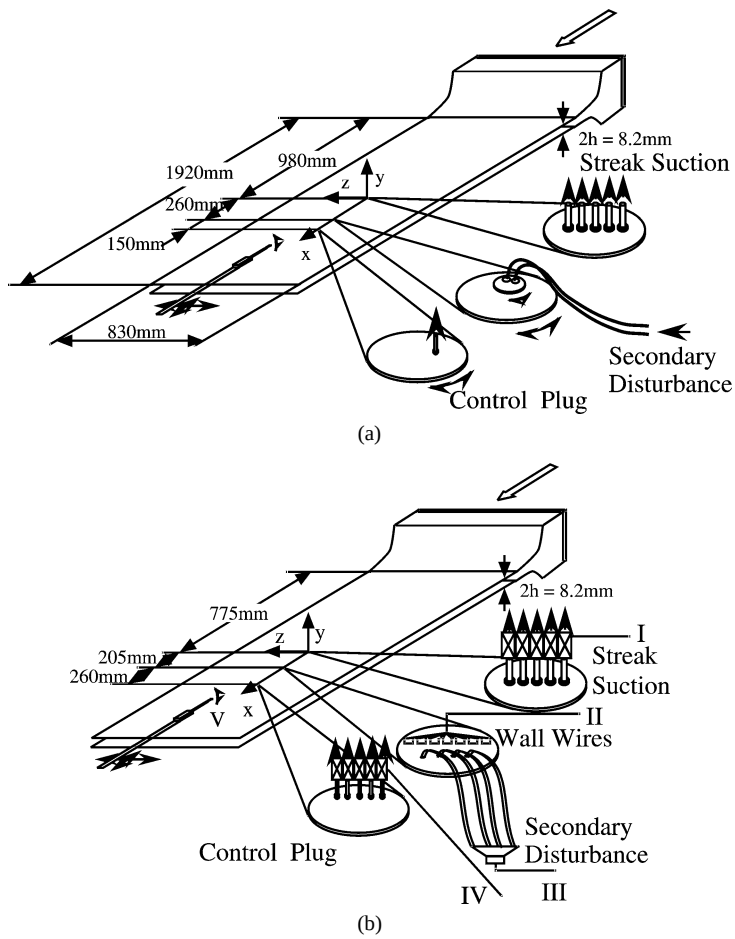

Fig. 1. Overview of experimental setup for active streak control (a) and reactive control (b).

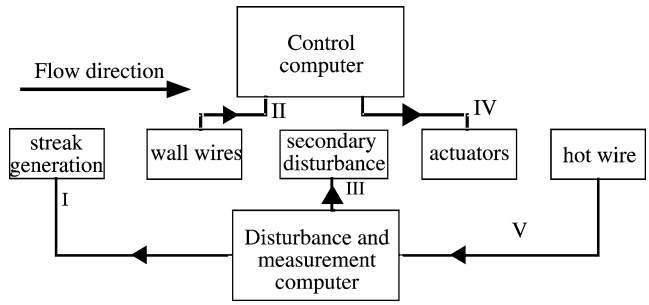

Fig. 2. Block diagram of the experimental setup for reactive streak control. The Roman numerals I–V refer to Fig. 1(b).

The dynamic pressure on the centreline was measured between a conical total-pressure tube inserted from the open downstream end of the channel and a static-pressure hole in the channel wall at the streamwise position of the conical tube. The maximum velocity in the channel was just above 13 m/s, corresponding to a Reynolds number of 3500. With no external disturbances applied, the flow was laminar at this Reynolds number.

The streamwise velocity was measured utilizing constant temperature hot-wire anemometry. The single hot wire used could be traversed to any position in the flow field where streaks were present (with stepper motors in the y- and z-directions and manually in the x-direction). Fast and reliable calibration of the hot wire was obtained by using the parabolic laminar velocity profile in the channel.

2.2. Disturbance generation

2.2.1. Continuous suction control

Streamwise streaks were created by localized suction from slots in the upper channel wall. Five streamwise-oriented slots, each with the dimensions 15×1.5 mm^2, with a separation of 15 mm in the spanwise direction, created five high-speed streaks at the upper wall, with low-speed streaks between them. The streaks were created when high-speed air was moved towards the wall in order to replace the low velocity air removed by the suction slot. The position of the suction slot was 980 mm, or 239 half channel-heights, downstream of the channel inlet. The streak amplitude could be varied and in the present experiment, the velocity difference between the high and low-velocity region was 55% of U_{CL}. The streak generation is positioned at $x = 0$ and $z = 0$ corresponds to the centre of a low-velocity streak.

High quality earphone-speakers (Sony) were used in order to force the secondary instability of the streaks. The disturbance was introduced through two narrow holes, positioned symmetrically over the centre of the low-velocity streak at $y = 1$, $z = \pm 1.2$. The earphones were driven by a sinuousoidal signal from a signal generator. By applying the original disturbance signal to one of the earphones and either the same or the inverted signal to the other, symmetrical (same) or anti-symmetric (inverse) modes of the streak oscillation could be triggered. The forcing was positioned 285 mm, i.e., $70h$, downstream of the streak generation. At the forcing position, the streaks had reached their maximum amplitude and were in a laminar, slowly decaying, phase.

2.2.2. Reactive control

In order to create time-dependent disturbances to be tackled by the reactive control system, solenoid valves were used to turn each high-speed streak on and off individually. The valves were controlled by the computer and the pattern with which the valves were turned on and off could be chosen as either predetermined or random. For the results reported here, a fixed pattern was used.

To fully complete the experimental simulation of time-dependent disturbances in a real boundary layer subjected to free-stream turbulence, not only the streaks themselves have to be time-dependent, but also the forcing of the secondary instability. This was done by using a number of spanwise oriented slots (0.5 mm wide in the streamwise and 10 mm long in the spanwise direction, respectively), connected to speakers creating a blowing/suction action through the slot. The speakers were driven by band-pass filtered (50–500 Hz) white-noise signals. The original signal and its reverse (since the signal is random, a phase shift is not possible) were connected to different slots, so that symmetric as well as anti-symmetric forcing was obtained. This forcing simulates the forcing by free-stream turbulence on streaks in a real boundary layer. With repeated and synchronized disturbance signals, ensemble averaging could give information from the whole flow field.

2.3. Control system

2.3.1. Continuous suction control

The objective of the control was to affect the low-speed streaks by localized suction and thereby reduce the growth of the secondary disturbance introduced by the earphones. The control suction was established through a 0.5 mm hole situated off-centre in a circular plug 85 mm ($21h$) downstream of the earphones forcing the secondary disturbance. In non-dimensional coordinates, the default control position was $(x_a, y_a, z_a) = (90, 1, 0)$. When rotating the plug, the off-centre hole moved in the spanwise direction so that the spanwise position of the hole, z_a (a for actuation), was altered. The flow through the control-suction hole was maintained by a small vacuum cleaner. It was around 0.25 l/min and was measured by a thermal mass-flow meter.

2.3.2. Reactive control

For reactive control, time-dependent localized suction was used to control the randomly occurring disturbances. In order to gain experience in control-system design, and to study the use of different control-algorithm parameters, the control system was complemented with sensors sensing the streamwise shear-stress at the wall and fast (300 Hz) solenoid valves for turning the control suction on and off. The sensors were platinum wall wires, 2.5 μm in diameter and 0.5 mm in length, welded to prongs, which were flush with the wall. The wires were bent, so that the centre of the wires was positioned 25–50 μm above the wall. The wall wires were not calibrated. However, the fluctuations of the output voltage from the wall wires were found to be close to linearly related to the shear-stress fluctuations by comparing the output voltage with the velocity measured by the hot wire when positioned close to the wall wire.

The spanwise positions of the sensors and actuators are shown in Fig. 3. As can be seen, the sensors are positioned with a spanwise separation of $\lambda/2$, with λ being the spanwise wavelength of the streaks. The actuators are positioned over the known positions of low-velocity streaks. The reaction time of the control system from sensing via processing to actuator output was 10–15 ms, most of which was the time for full control-suction strength to be established after the control-suction valves were opened.

The control algorithm was based on the spanwise difference of the streamwise shear. The shear-stress difference between two adjacent sensors, Δ_i, was calculated as

$$\Delta_i(t) = \frac{s_i(t) - s_{i+1}(t)}{\Delta_{\max}} \tag{1}$$

with

$$\Delta_{\max} = \max\left|s_i(t) - s_{i+1}(t)\right|, \quad i = 1, \ldots, 6. \tag{2}$$

The quantity $s_i(t)$ is the normalized shear stress signal measured by sensor i and $\Delta_{\max}$ is the maximum difference that can be created by the streak suction. Whenever

$$\left|\Delta_i(t)\right| > \Delta_{\text{thr}} \tag{3}$$

with Δ_{thr} being a threshold value between 0 and 1, the control suction was turned on at the spanwise position of low shear after a time delay τ. When $|\Delta_i|$ decreased below the threshold, control was turned off, again with the delay τ. The two extreme cases of Δ_{thr}, 0 and 1, correspond to continuous suction and no suction, respectively.

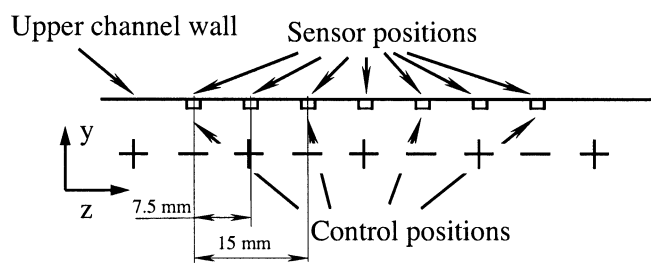

Fig. 3. Spanwise positioning of sensors and actuators. In the real setup the wire prongs are flush with the wall.

3. Results

3.1. Continuous suction control

This part reports results where continuous localized suction is performed below a low-velocity streak, and it is shown that the breakdown can be delayed. For each measurement station, measurements were performed twice: first without and then with control applied, in order to keep experimental conditions as constant as possible and allowing a direct comparison for the case with and without control. All measurements reported in the present section were made with a centreline velocity of 7.6 m/s giving a Reynolds number of 2000. The Reynolds number was chosen to match Elofsson et al. [12]. The case with no control applied is referred to as the reference case.

The reported data was measured at $y = 0.6$, i.e., $0.4h$ from the upper wall. The previous study by Elofsson et al. [12] shows that the secondary disturbance has its maximum amplitude at this height. The secondary disturbance was introduced at $x = 70$ and the frequency (260 Hz) was in the range of the most unstable frequencies for the present streaks. The earphones were situated symmetrically over the centre streak (at $z = \pm 1.2$) and the forcing was anti-symmetric. Elofsson et al. [12] found that even with the symmetric triggering, the anti-symmetric mode appears and grows faster.

In Fig. 4, the mean velocity (a), (c) and amplitude of the secondary instability (u_{rms}) (b), (d) are shown in the xz-plane at $y = 0.6$. The two left graphs, (a) and (b), show the flow field with no control applied whereas (c) and (d) to the right show the flow field for the case with control applied. Note that the x-coordinate is compressed with a factor 2.5 compared to the z-coordinate. The measurement grid consists of 10 positions in x and 45 in z. At each measurement point, 32 768 velocity values were sampled at a sampling rate of 3 kHz. The average velocity, calculated as the average over $90 < x < 180,\ -3.6 < z < 3.6$ (two wavelengths in the spanwise direction), is subtracted why the streaks appear as regions of positive and negative velocity (Fig. 4 (a) and (c)). The maximum peak-to-peak amplitude of the velocity streaks is larger than 50 % of the centreline velocity in the case with no control suction. Comparing Fig. 4 (a) and (c), it is seen that in the case with control applied, (c), the streaks are of lower amplitude as compared to the reference case. Also, the controlled streaks are more or less unchanged throughout the measurement region, in contrast to the situation in (a), where the streaky structure is less apparent for the downstream part of the measurement area.

The contours of Fig. 4 (b) and (d) indicate the disturbance level without and with control applied. Note that the disturbance contours are logarithmic so that equidistant contours show exponential growth. With no control applied, the downstream ($x > 145$) development of the secondary disturbance, Fig. 4(b), shows saturation as well as spreading of the secondary instability to neighboring streaks, with the largest amplitude between high and low-velocity regions. Even further downstream, $x > 160$, the *rms*-level is smeared out in the central part which is an indication of transition. Another sign of transition is seen in the mean-velocity distribution, becoming increasingly homogeneous in the spanwise direction.

If, however, the control suction is applied below the central low-velocity streak at $x = 90$, Fig. 4(d) shows that the control suction introduces some local disturbances at $x = 90-110$. Further downstream, the growth of the secondary instability is seen. As for the reference case with no control applied in Fig. 4 (b), the disturbance has its maximum value between the region of high and low-velocity. The contour levels are the same in Figs. 4 (b) and (d), and it is seen that the disturbance growth in the streamwise direction as well as the spreading of the secondary instability in the spanwise direction substantially decreases with the control turned on. The signs of laminar-turbulent transition in Fig. 4 (a) and (b): disappearance of the streaks and the

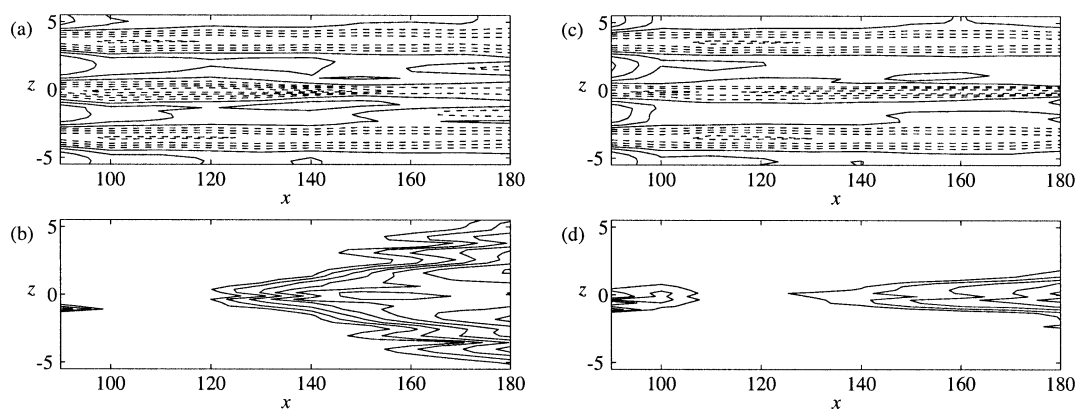

Fig. 4. Mean velocity disturbance (a), (c) and velocity *rms* (b), (d) of the streaks in the channel with (a), (b) and without (c), (d) control applied. The velocity contours in (a) and (c) are $\pm 5\%$, $\pm 15\%$ of U_{CL} after subtraction of the mean velocity in the region $90 < x < 180,\ -3.6 < z < 3.6$; the *rms*-contours in (b) and (d) are logarithmic 1.75%, 2.5%, 3.8%, ... of U_{CL}. Data taken at $y = 0.6$.

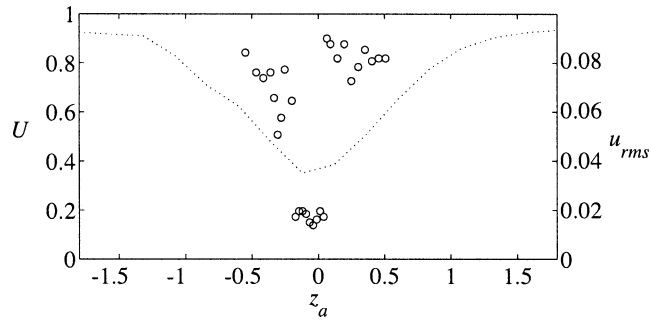

Fig. 5. Velocity fluctuations as a function of actuation position, z_a, $(\cdots)$ U at $(x, y, z) = (145, 0.6, z_a)$ (left scale) and $(\circ)$ u_{rms} at $(x, y, z) = (145, 0.6, 0.5)$ with control suction applied at z_a (right scale).

saturation of the *rms*-level are not present in Fig. 4 (c) and (d). This indicates that the control suction decreases the growth of the secondary instability and thus delays the process of breakdown to turbulence of the streak.

In the experiment above, the suction was applied directly below a low-speed streak. In a realistic situation, where disturbances appear randomly, this will not be the case. Therefore the dependence of the control effect on the spanwise control position was studied. By rotating the control plug the control suction hole could be moved in the spanwise direction. As a diagnostic, the disturbance level at a fixed position downstream of the control, in this case $(x, y, z) = (145, 0.6, 0.5)$, was measured. This position was chosen because, for the reference case, the disturbance distribution has a maximum there (see Fig. 4(b)). At this position, the flow is transitional with no control applied. In Fig. 5 the disturbance level at this position is shown with various z_a. In the figure, the spanwise velocity profile at the streamwise position of control and z-values corresponding to z_a is shown. From the figure it is obvious that for successful control to be achieved, the suction can only be applied to a narrow region close to the centre of the low-velocity streak. The width of the region where control is to be applied is seen to be $0.25h$, corresponding to less than 1 mm in the physical setup.

Increasing the strength of the control suction, the width of the region for which control is successful becomes narrower. Decreasing the suction strength, the control effect rather abruptly disappears. If the flow rate through the control suction hole is non-dimensionalized by the centreline velocity and the area where laminar flow is maintained with control as compared to that without control, a non-dimensionalized suction coefficient can be obtained as $C_q = q/AU_{CL}$ where C_q is the suction coefficient, q the flow rate, and A the controlled area (the area where transition is inhibited by the control). In the present case the area is a triangle with corners in $(x, z) = (150, 0)$, (180, 3) and (180, -3) (see Fig. 4), and a suction coefficient less than 4×10^{-4} is obtained with a flow rate of 4.2 cm^3/s (the approximate flow rate used in the experiments). The amount of fluid withdrawn from the flow by the control suction is about 1.3% of the flow through the part of the channel occupied by the streak (one streak wavelength times half the channel height). In the current experiment, the control suction was applied fairly far downstream of the streak generation. It is believed, and indicated in boundary layer experiments by Bakchinov et al. [16], that the suction necessary for successful control decreases if the control suction is applied further upstream. In Fig. 6 the velocity and disturbance distributions without control applied are studied in detail at each streamwise position.

In Fig. 6(a)–(e), the mean velocity profile is seen to be more or less constant. However, in (f)–(i), an increasing modification is seen to appear. Since this modification starts to appear right after the *rms*-value reaches its maximum in the centre at $x = 150$ (Fig. 6(f)), it is believed that transition to turbulence plays an important part in the modification of the mean velocity profiles. Even further downstream, it is seen that the mean velocity in the region $-3.6 < z < 3.6$ increases, indicating development of the fuller turbulent velocity profile. It is also seen that the smearing of the mean velocity profile mentioned in the discussion of Fig. 4 is actually a "streak doubling". In Fig. 6, the onset of the secondary instability between the regions of high and low-velocity is clearly seen. As the secondary instability spreads in the spanwise direction, it is seen that it first appears at the new inflection point arising due to the streak doubling (see Fig. 6(g) at $z = -1$) and as it grows, the maximum moves towards the centre of the newly created low-velocity streak, similar to the behaviour of the original, central low-velocity streak from Fig. 6(c)–(f).

A similar, but delayed, behaviour is seen in the case with control applied in Fig. 7. The control makes a small modification of the mean velocity distribution, as compared to the case without control applied (compare the dashed line in Figs. 6 (no control) and 7 (with control) (a)–(d)). The control suction is seen to increase the minimum velocity from 0.3 to 0.5, thus decreasing the maximum value of $\partial U/\partial z$ and the amplification of the secondary instability.

From previous figures it is clear that the growth of the secondary instability decreases for the continuous suction control case. In Fig. 8 the maximum of the *rms*-level for the two cases are compared. For each of the two cases, the *rms*-level has been normalized with its minimum value, obtained at $x = 110$. The decreased growth of the secondary instability in the controlled case is clearly seen. The two lines in the figures are the least-square fits to the N-values in the region where the exponential growth of the secondary disturbance occurs ($x = 120-140$ in the case of no control and $x = 110-180$ in the case with control

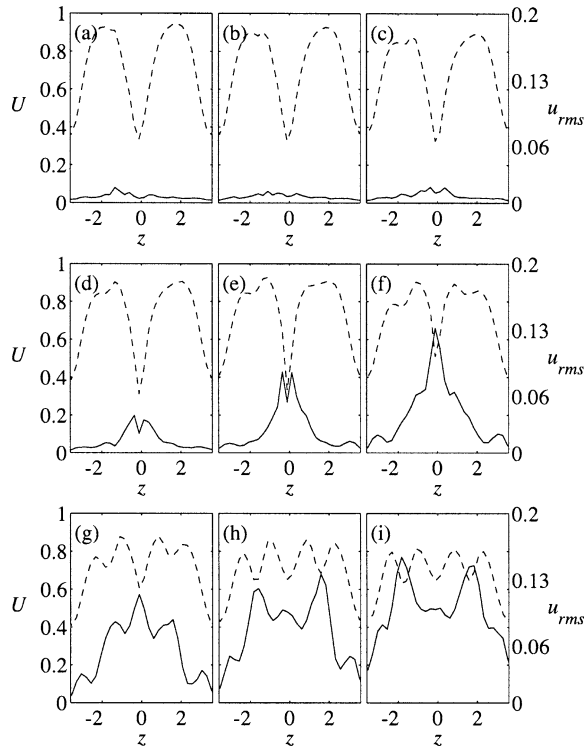

Fig. 6. Spanwise mean velocity ($\cdots$, left scale) and distribution (–, right scale) distribution at (a) $x = 100$ to (i) $x = 180$ *without* control applied. All data are taken at $y = 0.6$.

applied). From the figure it is obvious that the control decreases the disturbance growth. The logarithmic growth factor becomes 0.082 without and 0.029 with control applied, i.e., the growth factor is smaller by a factor of 3 in the controlled case.

3.2. Reactive control

All results in this section were obtained at a Reynolds number of 3300, corresponding to a centreline velocity of 12.5 m/s. This higher Reynolds number was chosen in order to get an illustrative, positive control result with a reasonable control suction rate.

Fig. 9 shows the streaks generated by turning the streak suction on and off. For the figure, a predetermined streak pattern has been used in order to create the streaks, so that repeated measurements give a picture of the flow pattern. As can be seen, elongated structures are created, with varying amplitude and length. The maximum peak-to-peak amplitude of the disturbances is approximately 65%, in the region of the values seen by Westin et al. [26] in measurements from a boundary layer subjected to FST prior to breakdown. The measurements shown in Fig. 9 were done without artificial forcing of the secondary instability. It is seen that the resulting streak pattern is of rather varying amplitude, despite the fact that when the suction is turned on, the suction velocity is constant. It is also seen that depending on whether one single or two neighboring streaks are turned on, the structures appear at different spanwise positions. In order to generate laminar structures such as the ones seen in Fig. 9, care has to be taken so that the streamwise gradients of the velocity, $\partial U/\partial x$ (corresponding to $\partial U/\partial t$ in Fig. 9), do not become too large at the leading and trailing edges of the disturbance. The leading edge of a high-velocity structure and the trailing edge of a low-velocity structure are most critical, since the high velocity tends to catch up with the slower fluid in front of it and thereby sharpen the gradients. For a low-velocity structure the same is valid for the faster fluid behind it and the trailing edge of the structure.

Velocity traces from $(x, y, z) = (200, 0.2, 0)$ with triggering of the secondary instability are shown in Fig. 10. In Fig. 10(a), the velocity with no control applied is shown, showing two low-velocity streaks passing the hot wire ($0.2 < t < 0.45$ and $t > 0.65$). It is seen that the low-velocity streaks oscillate strongly during some periods, the strongest for $0.4 < t < 0.43$ and $0.7 < t < 0.75$. This is possibly due to the receptivity of the streaks; whenever the forcing signal triggers an unstable frequency, the resulting disturbance will grow, giving rise to large amplitude velocity oscillations further downstream. In Fig. 10 it is also seen that the secondary disturbance only appears when there is a low-velocity streak present. For the periods when the velocity is undisturbed (12 m/s), there are no signs of high frequency disturbances (observed throughout the full time records). With the

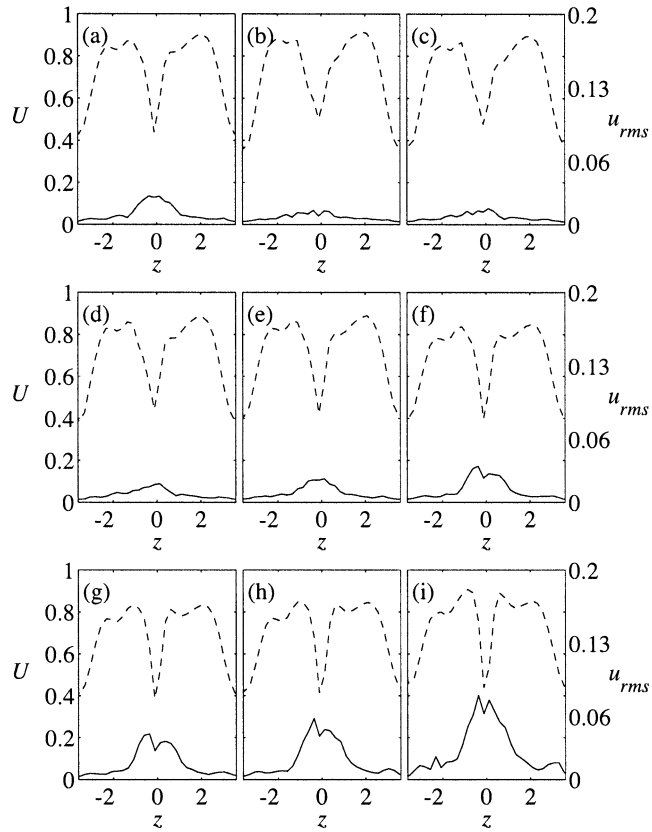

Fig. 7. Same as for Fig. 6 but *with* control applied.

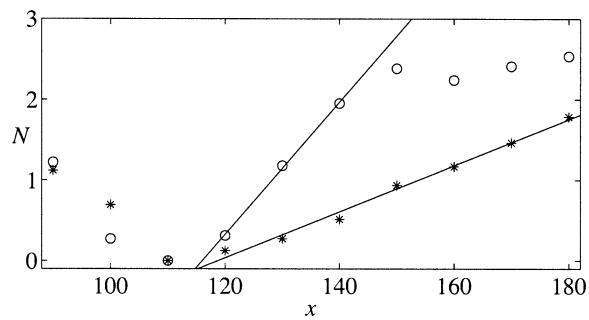

Fig. 8. Growth of the secondary disturbance without (∘) and with (∗) control applied. The lines have slopes of 0.082 and 0.029, respectively. N is calculated as $\ln(u_{rms}/u_{rms,\min})$. The disturbance level is choosen as the maximum of u_{rms} in the spanwise direction at $y = 0.6$.

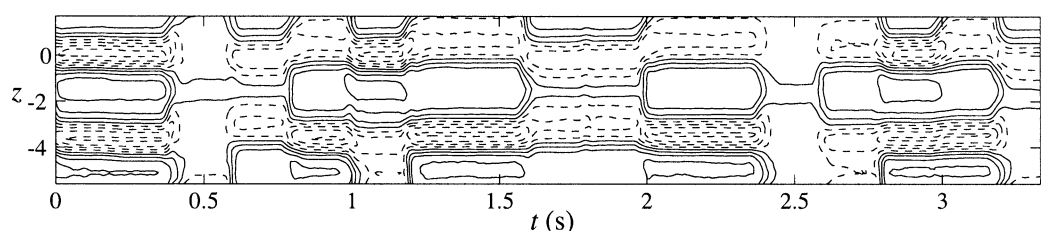

Fig. 9. Streak produced at $(x, y) = (200, 0.6)$ by turning the streak suction on and off. A time period δt of 1 s corresponds to approximately $\delta x = 2000$, why the time axis should be stretched 150 times in order to get a physical aspect ratio of the disturbances. Contour spacing is ±10% of U_∞ with negative contours dashed.

control applied, Fig. 10(b), it is seen that the amplitude of the low velocity disturbance has decreased, as well as the number, amplitude and length of the high-frequency oscillations. The forcing conditions were the same during the two measurements shown in Fig. 10.

In Fig. 10 (c) and (d), the portions between the crosses in Fig. 10 (a) and (b) have been high-pass filtered so that only the oscillations due to the secondary instability of the streaks remain; the low-frequency passings of the streaks are filtered out. It is seen that the large amplitude, high frequency oscillation is stronger and more intermittent/turbulent in the case with no control applied as compared to the controlled case.

During the measurements, it was desirable to have an easy-to-calculate indicator of whether the flow was disturbed/turbulent or laminar. In order to obtain such a measure the *rms* of the high-pass filtered ($f > 50$ Hz) velocity signal at the centre of the low-velocity streak was calculated. The height $y = 0.2$ was chosen since the high-frequency oscillations at this height were

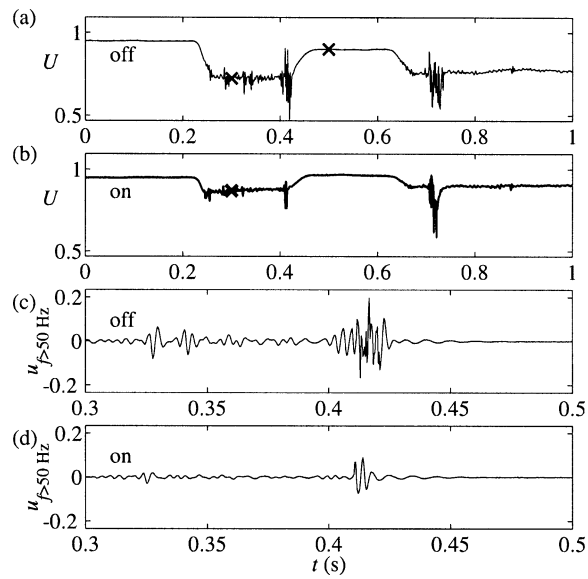

Fig. 10. Velocity traces from the setup with triggering of the secondary instability. In (a) and (c) no control is applied, in (b) and (d) reactive control was applied so that the control suction was turned on during the passing of the low-velocity streak in question. In (c) and (d), the signal has been high-pass filtered at 50 Hz in order to isolate the high frequency oscillations. The position is $(x, y, z) = (200, 0.2, 0)$. In the controlled case the controller parameters are $\tau = 0$ and $\Delta = 0.6$.

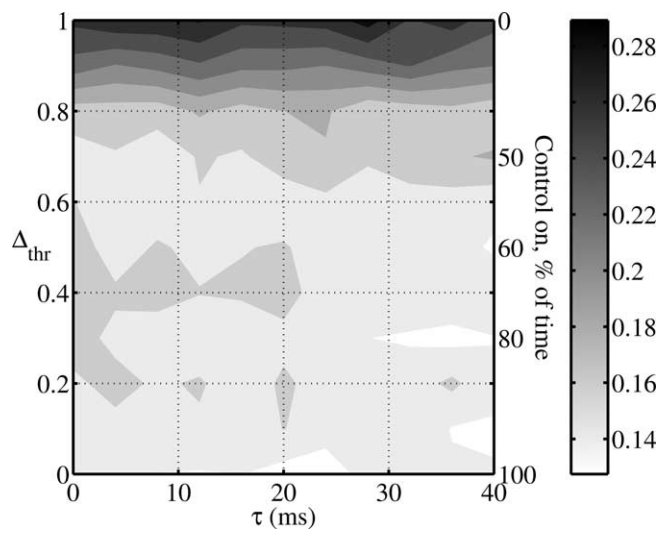

Fig. 11. Control effect for various control parameters. Hot-wire position is $(x, y, z) = (200, 0.2, 0)$.

found to be the best indicator of whether the flow is disturbed/turbulent or not. Closer to the wall, e.g., at $y = 0.6$, as used in the previous section, it is not possible to distinguish a turbulent flow from a laminar one on the basis of the *rms*. At $y = 0.6$ the maximum *rms*-value is namely obtained for an intermittent transitional flow; at $y = 0.2$ the maximum *rms* is obtained for a fully developed turbulent flow.

The control effect for different controller parameter settings is shown in Fig. 11. The two parameters are the threshold value of the streak detection, Δ_{thr} and the time delay from detection to actuation, τ, as discussed in Section 2.3. The control effect is measured as the high-frequency oscillation at $(x, y, z) = (200, 0.2, 0)$. The total number of parameter settings shown in the figure is 121 (11×11). It is clearly shown that for $\Delta_{\text{thr}} < 0.7$ there is a strong reduction of the high frequency fluctuations independent of the time delay and that the effect is insensitive to the exact value of Δ_{thr}. With $\Delta_{\text{thr}} = 0.6$ the suction is turned on approximately 50% of the time. This coincides with the time during which the low-speed streaks are turned on at their maximum amplitude, and indicates that control has to be applied for all times at which streaks exist for the control to be efficient. The exact timing of the control is however less critical.

4. Summary

The present study is part of a larger effort in order to understand, predict and control transition induced by free-stream turbulence. Streaks, modeling the disturbances in a boundary layer subjected to free-stream turbulence, were created in a channel flow. Successful delay of transition was obtained, probably by decreasing the spanwise velocity gradient, $\partial U/\partial z$, which drives the inviscid inflection-point instability.

Similar effects have also been demonstrated by Myose and Blackwelder [14] (Görtler vortices) and Egami and Kohama [27] (crossflow vortices). As in the present study, they both report transition delay obtained by localized suction applied at the position of low-velocity. We have demonstrated that the spanwise position at which control suction is applied has a large impact on the control effect. The control suction has to be applied at a narrow region close to the centre of a low-velocity streak in order to obtain the control effect.

A measure of the control effort is the suction coefficient, $C_q = V/U_\infty$, where V is the suction rate averaged over the wall area. Classical results reviewed by Gad-el-Hak [28] show that no T-S waves will be amplified if the suction coeffcient is 1.18×10^{-4} in the case of evenly distributed suction. However, if free-stream turbulence induced transition is to be inhibited, recent experiments by Fransson [29] show that the suction coefficient has to be increased substantially over this value if transition is to be avoided. With a free-stream turbulence level of 1.6%, a suction coefficient of 2.5×10^{-3} was needed to avoid transition. For localized actuation, the suction coefficient at the location of the control is much higher, but a more relevant suction coefficient is obtained if the suction is averaged over the area where the control action has the desired effect. The effective suction area has been obtained in various ways. Myose and Blackwelder [14] used the area from the leading edge to the suction position. Other investigators (e.g., Gad-el-Hak and Blackwelder [15] and Egami and Kohama [27], calculated the area from the streamwise length and spanwise separation of their suction slits. The well-defined disturbances and detailed measurements of the control effect used in the present experiment gave the possibility to calculate the suction coefficient based on the area over which the control suction inhibits transition (i.e., the area laminarized by the control). With such a definition of the effective suction area, the suction coefficient obtained from the present experiment (4×10^{-4}) is less than 20% of the critical value obtained by Fransson [29].

Control experiments on time-varying streaks, randomly forced, have also been reported. Such disturbances are similar to disturbances induced by FST laminar boundary layers. A reactive control system was designed and evaluated. As in the previous case, transition was delayed by the control. The control system consisted of seven upstream wall-wire sensors, detecting the streamwise shear stress at the wall. Further downstream, suction through four streamwise slots, turned on and off by fast solenoid valves, was used in order to control breakdown to turbulence of the disturbances. As in the case with time independent streaks, transition delay was obtained by decreasing the growth of the secondary disturbance acting on the streaks. It was seen that if only the control suction was turned on for sufficiently long time periods, the timing, i.e., the delay between sensing a structure and proper actuator output, did not have a large impact on the control effect.

This reactive control system should be able to control similar random streaky structures in a boundary layer in a wind tunnel over an area which comprises several streaky structures in the spanwise direction. As compared to earlier experiments on reactive transition control by localized suction, the present study presents more detailed measurements of the control effect and employs a larger number of sensors and actuators. Visualization results of Matsubara and Alfredsson [5] show that the structures seen in grid-generated FST induced transition appear and disappear at various positions, but once created, a disturbance move only slowly in the spanwise direction during its development. Such a behaviour highly simplifies control, since a once detected structure basically convects straight downstream while growing/decaying.

In the reactive control experiments, it was not possible to vary the streamwise position of the control, also the current control was applied on already formed streaks. However, experiments in a boundary layer by Bakchinov et al. [16], indicate

that applying the control as close as possible to the position at which the disturbance is introduced gives the most reduction in growth of transiently growing structures (such as the streaks in the present experiment). This means that a control system to be used in a real boundary layer has to identify disturbances potentially leading to large transient growth and transition at an early stage, indicating the need for adaptive controllers with system identification. Such controllers have been used to control turbulence by Rathnasingham and Breuer [19]. It is our intention to use the experience gained from the experiments reported here together with earlier results to build a multi-input/multi-output reactive control system and use it to delay transition in boundary layers subjected to free-stream turbulence.

Acknowledgements

The work of earlier experimentalists (especially Dr. Per Elofsson and Dr. Mitsuyoshi Kawakami) in the channel gave the present project a flying start! Mr. Marcus Gällstedt is an excellent tutor in designing and constructing experimental equipment. Dr. Jens Österlund gave some invaluable time-saving advice on the manufacturing of wall wires. Dr. Johan Westin carefully read an early version of the manuscript. Michaela Agoston proof read the manuscript. The persons mentioned above are all acknowledged. So is financial support from VR (the Swedish Research Council) and KTH (Royal Institute of Technology, Stockholm).

References

[1] D.M. Bushnell, C.B. McGinley, Turbulence control in wall flows, Ann. Rev. Fluid Mech. 21 (1989) 1.
[2] M. Gad-el-Hak, Modern developments in flow control, Appl. Mech. Rev. 49 (1996) 365.
[3] T.R. Bewley, P. Moin, R. Temam, DNS-based predictive control of turbulence: an optimal benchmark for feedback algorithms, J. Fluid Mech. 447 (2001) 179.
[4] J.M. Kendall, Experiments on boundary-layer receptivity to freestream turbulence, AIAA-paper 98-0530, 1998.
[5] M. Matsubara, P.H. Alfredsson, Disturbance growth in boundary layers subjected to free stream turbulence, J. Fluid Mech. 430 (2001) 149.
[6] R.G. Jacobs, P.A. Durbin, Simulations of bypass transition, J. Fluid Mech. 428 (2001) 185.
[7] K.M. Butler, D.F. Farrell, Three dimensional optimal perturbations in viscous shear flow, Phys. Fluids A 4 (1992) 1637.
[8] P. Andersson, M. Berggren, D.S. Henningson, Optimal disturbances and bypass transition in boundary layers, Phys. Fluids 11 (1999) 134.
[9] P. Luchini, Reynolds number independent instability of the boundary layer over a flat surface: optimal perturbations, J. Fluid Mech. 404 (2000) 289.
[10] A.V. Johansson, P.H. Alfredsson, J. Kim, Evolution and dynamics of shear-layer structures in near-wall turbulence, J. Fluid Mech. 224 (1991) 579.
[11] F. Waleffe, Hydrodynamic stability and turbulence: beyond transients to a self-sustained process, Stud. Appl. Math. 95 (1995) 319.
[12] P.A. Elofsson, M. Kawakami, P.H. Alfredsson, Experiments on the stability of streamwise streaks in plane Poiseuille flow, Phys. Fluids 11 (1999) 915.
[13] P. Andersson, L. Brandt, D.S. Henningson, On the breakdown of boundary layer streaks, J. Fluid Mech. 428 (2001) 29.
[14] R.Y. Myose, R.F. Blackwelder, Control of streamwise vortices using selective suction, AIAA J. 33 (1995) 1076.
[15] M. Gad-el-Hak, R.F. Blackwelder, Selective suction for controlling bursting events in a boundary layer, AIAA J. 27 (1989) 308.
[16] A.A. Bakchinov, M.M. Katasonov, P.H. Alfredsson, V.V. Kozlov, in: H.F. Fasel, W.S. Saric (Eds.), IUTAM Symposium on Laminar-Turbulent Transition, Springer-Verlag, Heidelberg, 2000, pp. 159–164.
[17] K.S. Breuer, J.H. Haritonidis, M.T. Landahl, The control of transient disturbances in a flat plate boundary layer through active wall motion, Phys. Fluids A 1 (1989) 574.
[18] X. Fan, T. Herbert, J.H. Haritonidis, Transition control with neural networks, AIAA-paper 95-0674, 1995.
[19] R. Rathnasingham, K.S. Breuer, System identification and control of a turbulent boundary layer, Phys. Fluids 9 (1997) 1867.
[20] H. Rebbeck, K. Choi, Opposition control of near wall turbulence with a piston-type actuator, Phys. Fluids 13 (2001) 2142.
[21] S.A. Jacobson, W.C. Reynolds, Active control of streamwise vortices and streaks in boundary layers, J. Fluid Mech. 360 (1998) 179.
[22] H. Choi, P. Moin, J. Kim, Active turbulence control for drag reduction in wall-bounded flows, J. Fluid Mech. 262 (1994) 75.
[23] C. Lee, J. Kim, D. Babcock, R. Goodman, Application of neural networks to turbulence control for drag reduction, Phys. Fluids 9 (1997) 1740.
[24] C.-M. Ho, Y.-C. Tai, Review: MEMS and its applications for flow control, J. Fluids Engrg. 118 (1996) 437.
[25] L. Löfdahl, M. Gad-el-Hak, MEMS applications in turbulence and flow control, Prog. Aerospace Sci. 35 (1999) 101.
[26] K.J.A. Westin, A.V. Boiko, B.G.B. Klingmann, V.V. Kozlov, P.H. Alfredsson, Experiments in a boundary layer subjected to free stream turbulence. Part 1. Boundary layer structure and receptivity, J. Fluid Mech. 281 (1994) 193.
[27] E. Egami, Y. Kohama, in: G.E.A. Meier, P.R. Viswanath (Eds.), IUTAM Symposium on Mechanics of Passive Active Flow Control, Kluwer Academic, Dordrecht, 1999, pp. 171–176.
[28] M. Gad-el-Hak, A.K.M.F. Hussain, Coherent structures in a turbulent boundary layer. Part 1: Generation of “artificial” bursts, Phys. Fluids 29 (1986) 2124.
[29] J.H.M. Fransson, P.H. Alfredsson, On the disturbance growth in an asymptotic suction boundary layer, J. Fluid Mech. 482 (2003) 51.